

PAPER

Fermi–Hubbard model on nonbipartite lattices: flux problem and emergent chirality

To cite this article: Wayne Zheng J. Stat. Mech. (2020) 073103

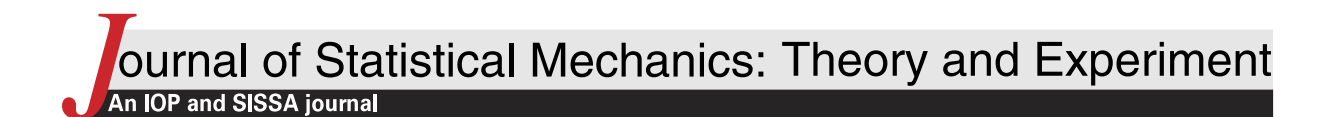
View the <u>article online</u> for updates and enhancements.



IOP ebooks™

Bringing together innovative digital publishing with leading authors from the global scientific community.

Start exploring the collection-download the first chapter of every title for free.



PAPER: Paper section: Quantum statistical physics, condensed matter, integrable systems

Fermi-Hubbard model on nonbipartite lattices: flux problem and emergent chirality

Wayne Zheng

Department of Physics, The Ohio State University, Columbus, Ohio 43210, United States of America

Received 26 February 2020 Accepted for publication 14 May 2020 Published 15 July 2020



Online at stacks.iop.org/JSTAT/2020/073103 https://doi.org/10.1088/1742-5468/ab99bf

Abstract. On several one-dimensional (1D) and 2D nonbipartite lattices, we study both free and Hubbard interacting lattice fermions when some magnetic fluxes are threaded or gauge fields coupled. First, we focus on finding out the optimal flux which minimizes the energy of fermions at specific fillings. For spin-1/2 fermions at half-filling on a ring lattice consisting of odd-numbered sites, the optimal flux turns out to be $\pm \pi/2$. We prove this conclusion for Hubbard interacting fermions utilizing a generalized reflection positivity technique, which can lead to further applications on 2D nonbipartite lattices such as triangular and Kagome. At half-filling the optimal flux patterns on the triangular and Kagome lattice are ascertained to be $\pm [\pi/2, \pi/2], \pm [\pi/2, \pi/2, 0]$, respectively (see the meaning of these notations in the main text). We also find that chirality emerges in these optimal flux states. Then, we verify these exact conclusions and further study some other fillings with the numerical exact diagonalization method. It is found that when it deviates from half-filling, Hubbard interactions can alter the optimal flux patterns on these lattices. Moreover, numerically observed emergent flux singularities driven by strong Hubbard interactions in the ground states— both in 1D and 2D—are discussed and interpreted as some kind of non-Fermi liquid feature.

Keywords: Hubbard and related model, quantum frustrated systems, rigorous results in statistical mechanics

Contents

1.	Introduction	2
2.	One-dimensional lattice 2.1. Non-interacting spin-1/2 fermions 2.2. Turn on Hubbard interactions 2.2.1. A numerical example 2.2.2. Generalized reflection positivity. 2.3. Flux singularity as a Luttinger liquid signature	6 6
3.	Two-dimensional lattices 3.1. A trial on a bowtie lattice	11 11 11
	 3.2.1. Half-filled free fermions coupled to a Z₄ gauge field	13
4.	Conclusion and discussion 4.1. Brief summary	17
	Acknowledgements	18
$\mathbf{A}_{]}$	ppendix A. One-dimensional free spinless fermions and the Jordan–Wigner transformation	18
A]	ppendix B. Half-filled spin-1/2 free fermions on a nonbipartite odd- -numbered ring	21
A j	ppendix C. Other fillings on the triangular lattice	22
A j	ppendix D. Review of the reflection positivity on a bipartite lattice	22
	References	2 4

1. Introduction

The Fermi-Hubbard model is very famous and important [1]. It has appealed to researchers for decades as the simplest route towards understanding strongly correlated fermionic quantum many-body systems. It is widely believed that the Hubbard model should be closely related to the essential ingredients of the Mott insulator and

high-temperature superconductivity [5, 8, 14, 41]. Numerically it has also been studied extensively [26, 39, 87]. Recently, interest in it has been simulated by ultracold atoms in experiments [30, 56, 79]. Here for our theoretical interest, we would like to mention and emphasize three related aspects.

Firstly, since the perturbation theory cannot always provide us with faithful and clear results if the Hubbard interactions are sufficiently strong, rigorous theorems can provide many great insights into the nonperturbative features of the Hubbard model [80]. A 1D bipartite lattice¹ has been solved exactly and it has been shown that there is no Mott transition [48, 49]. On 2D bipartite lattices at half-filling, Lieb settled the ground state's uniqueness and its total spin up to any finite repulsive Hubbard interaction [45]. If a hole is doped on 2D bipartite lattices, strong Hubbard interactions can induce an emergent Nagaoka ferromagnetism [60]. We notice that, both in 1D and 2D, the bipartiteness plays an important role in many of these significant theorems. It leads to a special kind of particle—hole transformation, where a minus sign only follows in one of the two bipartite subsets of the lattice sites. Moreover, quantum Monte Carlo can also avoid the severe sign problem due to the bipartiteness [57, 75]. Thus a natural question can be asked: why does the bipartiteness seem to be so essential here? What will happen if we lose it?

Secondly, without any doubt fermions and gauge fields can indeed emerge from very different strongly correlated bosonic quantum many-body systems [3, 7, 40, 44, 71]. The exactly solvable Kitaev honeycomb spin model is supposed to be the most convincing example, which equivalently turns out to be emergent free Majorana fermions coupled to a \mathbb{Z}_2 lattice gauge field [33]. These emergent gauge fields living on the lattice links can form magnetic fluxes, of which the corresponding effective magnetic field can be so strong that no experiment on Earth can realize it. The low-energy gauge fluctuations above the mean-field state turn out to be crucial, and even the topology of the gauge fields plays a significant role [2, 71, 72, 85]. In these kinds of fermion–gauge-field coupled systems, finding out the optimal flux pattern to minimize the ground state energy at zero-temperature or the statistical free energy at any finite temperature is called the flux problem. For Hubbard interacting fermions at half-filling, Lieb solved the flux problem on generic 2D bipartite lattices with the help of an elegant technique called reflection positivity [46, 54] (RP) which was first introduced in quantum field theory [65]. Lieb's result directly leads to the solution of Kitaev's honeycomb model. The optimal π -flux Dirac state on a square lattice has been observed numerically in a fermion—gauge-field coupled system [17]. It is used to serve as a good starting point to construct quantum spin liquids (QSLs) in the language of fermionic partons [81, 86]. Note that days earlier, high- T_c superconductivity was also found to be closely related to the flux issue [2, 35].

Thirdly, it is well known that the spin chiral operator $\chi \equiv \sigma_1 \cdot (\sigma_2 \times \sigma_3)$ can be expressed by the flux Berry phase ϕ acquired by fermions hopping along a closed plaquette [84]. To be specific, $\langle \chi \rangle \propto \sin \phi$, where ϕ is the flux threaded throughout the plaquette. For 2D bipartite lattices, the typical 0 or π -flux optimal states are nonchiral, where chirality $\langle \chi \rangle$ vanishes. Therefore, there does not exist persistent spin current around the plaquettes induced only by nonzero chirality.

¹ A bipartite lattice Λ is the one $\Lambda = A \cup B$, $A \cap B = \emptyset$ and $t_{ij} = 0$ if $i, j \in A$ or $i, j \in B$ [46], where t_{ij} is the fermion hopping amplitude.

In this sense, in this paper we would like to investigate Hubbard interacting fermions without bipartiteness any longer, to see its interplay with gauge fields and chirality. We obtained several new results analytically as well as numerically. The rest of this paper is organized as follows. In section 2, from noninteracting to interacting cases, 1D lattice fermions are investigated. The optimal flux for spin-1/2 fermions at half-filling on a nonbipartite odd-numbered ring is proved and verified numerically no matter whether the Hubbard interactions are present or not. In section 3, we generalize our technique to 2D and study the flux problem for the Hubbard model on 2D nonbipartite lattices. At half-filling, the optimal flux patterns for the triangular and Kagome lattices can be nailed down. However, when it deviates from half-filling, there are no rigorous analytical results anymore. Some numerical results are provided and discussed in both 1D and 2D. In particular, emergent flux singularities driven by strong Hubbard interactions are addressed and identified as non-Fermi liquid (NFL) features. In section 4, we finish with a brief summary and discussion.

2. One-dimensional lattice

2.1. Non-interacting spin-1/2 fermions

First, let us warm up by taking a look at the simplest case, namely fermions living on a 1D lattice, which are always assumed to form a ring. For two branches of nonrelativistic spin-1/2 free noninteracting fermions $\sigma = \uparrow, \downarrow$, they can be treated separately as

$$H_t = -\sum_{\sigma} \sum_{j=0}^{L-1} \left(t_{j,j+1} c_{j\sigma}^{\dagger} c_{j+1,\sigma} + \text{h.c.} \right).$$
 (1)

As usual, $j+1 \equiv (j+1) \mod L$. $\{c_{i,\sigma}^\dagger, c_{j,\sigma'}\} = \delta_{i,j}\delta_{\sigma,\sigma'}$ and $\{c_{i,\sigma}, c_{j,\sigma'}\} = \{c_{i,\sigma}^\dagger, c_{j,\sigma'}^\dagger\} = 0$ define the complex fermionic operators. $t_{i,j+1}$ is the Wannier hopping amplitude and $|t_{i,i+1}| = t = 1.0$ is set to be the energy unit throughout this paper. A magnetic flux ϕ can be added through appropriate boundary conditions such as $t_{N-1,0} = e^{-i\phi}$, while for the others $t_{j,j+1} = 1.0, j \neq L-1$. By a discrete Fourier transformation $c_j = \frac{1}{\sqrt{L}} \sum_k e^{ikj} c_k$, $H_t = -\sum_{\sigma}\sum_{k}(2 \cos k)c_{k,\sigma}^{\dagger}c_{k,\sigma}$, where $k = (2\pi l + \phi)/L$ is constrained by the boundary condition. $l \in \mathbb{Z}$. The ground state energy is determined by the band fillings given U(1) conserved particle numbers $N_{\uparrow,\downarrow}$, which is illustrated in figure 1. It is easy to check that when $N_{\uparrow} = N_{\downarrow} = 2n$, $n \in \mathbb{Z}_{+}$, the optimal flux takes $\phi_{\text{opt}} = \pi$. When $N_{\uparrow} = N_{\downarrow} = 2n + 1$, $n \in \mathbb{Z}_{+}$, the optimal flux is $\phi_{\text{opt}} = 0$. When $N_{\uparrow} = 2n$, $N_{\downarrow} = 2m - 1$, $n, m \in \mathbb{Z}_{+}$, the optimal flux should lie at some value between 0 and π to minimize the filling energy of these two branches of fermions. According to the discussion in appendix A, if we implement the Jordan-Wigner transformation on these two branches of fermions separately, different parities would lead to competition when it comes to minimizing the ground state energies by the natural inequality [63, 64]. Therefore, a chiral optimal flux can indeed emerge in such a scenario. Generally, this depends on $N_{\uparrow,\downarrow}$ and L as $\phi_{\mathrm{opt}} = \phi_{\mathrm{opt}}(N_{\uparrow}, N_{\downarrow}, L)$. The optimal flux in this scenario can be determined by certain transcendental triangular equations, which can be solved numerically. For example, if

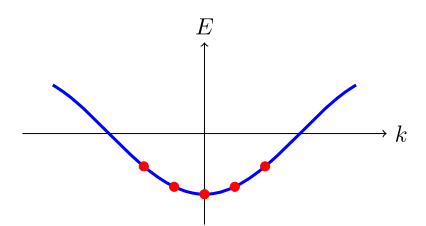


Figure 1. Band of free fermions in 1D.

 $N_{\uparrow}=2, N_{\downarrow}=1$, at a local minimum we have

$$2 \sin\left(\frac{\phi}{L}\right) = \sin\left(\frac{2\pi - \phi}{L}\right). \tag{2}$$

Say, L=5, here the optimal flux $\phi_{\rm opt} \simeq 1.9536$. However, we found that $\phi_{\rm opt}$ is very special when it comes to the half-filled case, which is independent of the odd L. For simplicity, here we only focus on the cases with a minimal $|S_{\rm tot}^z| = \frac{1}{2} |N_{\uparrow} - N_{\downarrow}|$ on a nonbipartite odd-numbered ring. Then we have the following lemma:

Lemma 1. For spin-1/2 free noninteracting fermions with a minimal $|S_{tot}^z|$ on a non-bipartite odd-numbered ring at half-filling, the optimal fluxes for the ground states are $\pm \pi/2$, which are independent of the lattice size L.

For a finite temperature, we can prove that

Lemma 2. For spin-1/2 free fermions on a ring lattice defined by equation (1), if the parities of particle numbers $N_{\uparrow,\downarrow}$ are identical, at finite temperature the optimal flux for the statistical free energy F is 0 or π depending on whether the parity is odd or even, respectively.

Proof. The basis for spin-1/2 fermions spanning the Hilbert space can be written in a specific representation [45] $|\alpha\rangle_{\uparrow}\otimes|\gamma\rangle_{\downarrow}$. Expanding the canonical partition function like

$$Z = \operatorname{tr}\left(e^{-\beta H_t}\right) = \lim_{M \to \infty} \operatorname{tr}\left[V^M(\phi)\right],\tag{3}$$

and

$$V(\phi) = 1 + \delta \sum_{\sigma} \left(\sum_{j=0}^{L-2} c_{j\sigma}^{\dagger} c_{j+1,\sigma} + e^{i\phi} c_{L-1,\sigma}^{\dagger} c_{0,\sigma} + \text{h.c.} \right), \tag{4}$$

where $\delta = \beta/M$. We rewrite $V^M(\phi) = \sum_{\alpha} X^{\alpha} = \sum_{\alpha} \prod_{\sigma} X^{\alpha}_{\sigma}$ when we rearrange the operator string by their spin indices. Then in this representation we have $\operatorname{tr}(\prod_{\sigma} X_{\sigma}) = \operatorname{tr}(X_{\uparrow}) \cdot \operatorname{tr}(X_{\downarrow})$. The lowest order nontrivial operator strings take the form $\operatorname{tr}(X_{\uparrow}) \cdot \operatorname{tr}(\mathbb{1}_{\downarrow}) + \operatorname{tr}(\mathbb{1}_{\uparrow}) \cdot \operatorname{tr}(X_{\downarrow}) = (-)^{N_{\uparrow}-1} \delta^{L} \mathrm{e}^{\mathrm{i}\phi} D_{\downarrow} + (-)^{N_{\downarrow}-1} \delta^{L} \mathrm{e}^{\mathrm{i}\phi} D_{\uparrow} + \mathrm{h.c.} = 2(-)^{N_{\uparrow}-1} D_{\downarrow} \delta^{L} \cos \phi + 2(-)^{N_{\downarrow}-1} D_{\uparrow} \delta^{L} \cos \phi$, where $D_{\uparrow,\downarrow} = C_{L}^{N_{\uparrow,\downarrow}}$ is the dimension of sub-Hilbert space corresponding to spin- \uparrow and $-\downarrow$ fermions, respectively. If N_{\uparrow} and N_{\downarrow} share the same parity, this very term maximizes just like the free spinless fermions discussed in

appendix A. A higher-order crossed term, such as $+2\delta^{2L}\cos(2\phi)$, maximizes at the same time. Once the partition function is maximized, free energy $F=-\frac{1}{\beta}\ln Z$ is minimized.

If the parities of N_{\uparrow} and N_{\downarrow} are different, at finite temperature there will be some competition in nontrivial terms such as $\pm 2(D_{\downarrow} - D_{\uparrow})\cos\phi$, which maximizes at 0 or π while the crossed term $-2\cos(2\phi)$ maximizes at $\pi/2$. Therefore, determining the optimal flux for the finite temperature free energy F is hard, and it might differ from the ground state.

2.2. Turn on Hubbard interactions

When the simplest kind of on-site interaction

$$H_U = U \sum_{j} n_{j\uparrow} n_{j\downarrow},\tag{5}$$

is turned on, we have the so-called Hubbard model [21, 28]. Its lattice Hamiltonian is given by $H = H_t + H_U$, where repulsive U > 0 is always assumed throughout this paper. The two branches of fermions gradually begin to interact and get entangled with each other as U increases from zero. On a bipartite ring lattice at half-filling, we can expect a four-fold degeneracy at most in terms of free spin-1/2 fermions, since every branch can contribute a two-fold degeneracy. Recall that Lieb told us that any finite Hubbard U can split this degeneracy, thereby leaving over a unique ground state [45]. For $N = N_{\uparrow} + N_{\downarrow} = 2n$, $n \in \mathbb{Z}_{+}$, the optimal flux for the ground state of the Hubbard model has been proved [61] to be 0 or π depending on the parity of N/2. Thus, it is quite meaningful to ask—on nonbipartite lattices—how the Hubbard interactions impact on the comprehensive features of free fermions, including the optimal flux problem.

2.2.1. A numerical example. Now let us carry out some numerical experiments by the exact diagonalization (ED) technique utilizing the ARPACKPP package [70]. They are quite simple but very helpful for obtaining some basic intuitions. Let us only consider three fermions $N_{\uparrow} = 2$, $N_{\downarrow} = 1$. On the one hand, L = 3 means half-filling, as illustrated in figures 2(a), (c) and (e) with increasing U/t = 0.0, 10.0, 100.0, both the ground state energy E_0 and finite temperature free energy F always minimize at $\phi_{\rm opt} = \pm \pi/2$. Not even a very strong Hubbard interaction affects the optimal flux value.

On the other hand, as we can see in figures 2(b), (d) and (f), L=5 means it is not half-filled. Firstly, the optimal flux for the ground state can be altered by the Hubbard interactions. There does not exist a universal optimal flux for the ground state of the Hubbard model when it is not half-filled. As U/t increases, the optimal flux for the ground state gradually shifts from the free fermions' $\phi_{\text{opt}} \simeq 1.9536$, which is approximately given by equation (2), to $2\pi/3$. In view of equation (2), it is interesting to realize that $2\pi/3$ is nothing but the optimal flux solution for the ground state of these free fermions when $L \to \infty$. These two limits $U \to \infty$ (fixed finite L) and $L \to \infty$ (U = 0.0) somehow arrive at the same optimal flux. This implies that in a quantum many-body system strong interactions can indeed drive some emergent nonpertubative features which cannot be understood by free or weakly interacting pictures. Secondly,

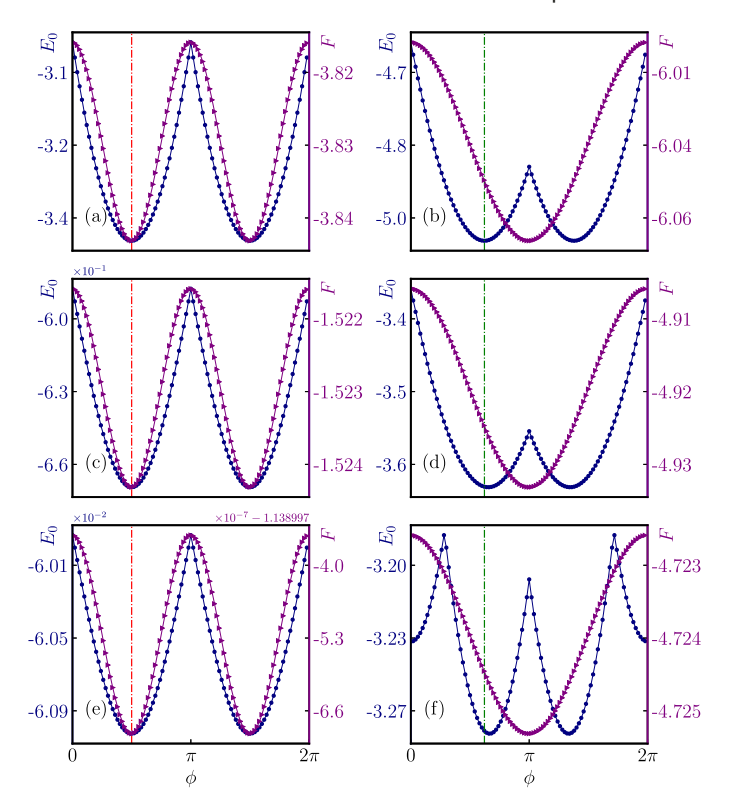


Figure 2. The ground state energy E_0 and the finite temperature free energy F of the 1D Hubbard model on a ring with fixed fillings $N_{\uparrow}=2, N_{\downarrow}=1$. Vertically from top to bottom, (a), (b), (c), (d) and (e), (f) denote U/t=0.0, 10.0, 100.0, respectively. Horizontally from left to right, (a), (c), (e) and (b), (d), (f) denote the lattice size L=3,5, respectively. Free energy is computed at $\beta=1.0$. The red dashed line marks the optimal flux $\phi_{\rm opt}=\pi/2$ for the ground state energy at half-filling. The green dashed line marks the optimal flux $\phi_{\rm opt}\simeq 1.9536$ for the ground state energy away from half-filling.

the finite temperature free energy F does not share the identical optimal flux with the ground state anymore; its optimal flux is located at $\phi = \pi$.

This numerical test, as well as the inspiration of lemma 1, give us faith that the optimal fluxes $\phi_{\rm opt} = \pm \pi/2$ always hold for the half-filled Hubbard model sitting on a nonbipartite odd-numbered ring. Half-filling seems to be a special fixed point. However, when it deviates from half-filling, it is much more complicated and there seemingly does not exist a universal conclusion.

2.2.2. Generalized reflection positivity. For the Hubbard interacting fermions, note that the RP technique can only be applied to a ring comprised of an even number of sites, hence resulting in the optimal flux of 0 or π . We succeeded in proving the following theorem with the aid of a generalized reflection positivity (GRP) technique.

Theorem 3. For a half-filled repulsive Hubbard model with a minimal $|S_{tot}^z|$ on a nonbipartite odd-numbered ring, at any finite temperature the optimal fluxes for its free energy F are $\pm \pi/2$.

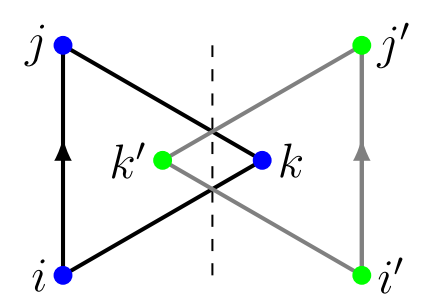


Figure 3. $\{i, j, k\}$ represents a half-filled Hubbard model living on a L = 3 ring lattice. $\{i', j', k'\}$ is merely a fictitious reflection of $\{i, j, k\}$ along the dashed line. Arrows mark the flux accumulating directions.

Proof. Here we take the simplest case to explain the GRP, as denoted by figure 3, where a half-filled Hubbard model lives on a triangle $\{i, j, k\}$. We would like to make a fictitious symmetric reflective copy of the system $\{i, j, k\}$ to $\{i', j', k'\}$. The same as discussed in reference [46], we are at liberty to choose the gauge as the flux is only added on the nonintersected links (i, j) and (i', j'). The other intersected links can be set to be $t_{ik} = t_{jk} = t$, although generally they are not Θ invariant, in which Θ is comprised of three steps: geometric reflection \mathcal{R} followed by a particle–hole transformation and a complex conjugation \mathcal{C} . If we regard these six sites as a whole system, according to Lieb's theorem [46], which is also reviewed in appendix D, the fulfillment of $\Theta(t_{ij}c_{i\sigma}^{\dagger}c_{j\sigma} + \text{h.c.}) =$ $-t_{j'i'}c_{i'\sigma}^{\dagger}c_{i'\sigma} + \text{h.c.} = -\mathcal{R}(t_{ij}c_{i\sigma}^{\dagger}c_{j\sigma} + \text{h.c.})$ leads to the maximum of the partition function of the Hubbard model. Note that $\{i', j', k'\}$ is merely a fictitious reflective image of the original system. If we want to separate the whole system and view them as two equivalent ones, we should make another following complex conjugation $t_{i'j'} = -t_{ij} \xrightarrow{\mathcal{C}} -t_{ij}^* \equiv t_{ij}$, which means t_{ij} is pure imaginary, and thereupon a $\pi/2$ flux is threaded through the triangle. Note that the second complex conjugation carried out here is to flip the flux direction of the reflective mirror system $\{i,j,k'\}$ back so as to match the original system $\{i, j, k\}$. It is easy to utilize our GRP for other ring lattices with odd-numbered sites L>3 as every nonintersected link contributes a $\pm\pi/2$ gauge flux. When the partition function is maximized, the free energy F is minimized.

In addition, we have some remarks.

(a) We think that it is dangerous to rashly deduce the ground state properties so as to let $\beta \to \infty$. A possible example is illustrated in figures 2(b), (d) and (f), where the thermal free energy does not share the same optimal flux with the ground state when it deviates from half-filling. There possibly exists a phase transition when the temperature jumps from any finite value to zero. However, for the half-filling, this somehow turns out to be safe such as the half-filled examples numerically shown in figures 2, 5 and 10. There the ground state energy always shares the identical optimal flux with the corresponding finite temperature free energy, at least speaking in terms of these numerical samples. We think it should have something to do with the coincidence implied by lemma 1, which suggests that a half-filled nonbipartite odd-numbered ring happens to be an unrenormalized fixed point, where the optimal

flux cannot be altered and renormalized by the Hubbard interactions any longer. Let us take a closer look at the finite temperature partition function of the 1D Hubbard model away from half-filling. Still suppose the basis spanning the Hilbert space is written in the representation $|\alpha\rangle_{\uparrow} \otimes |\gamma\rangle_{\downarrow}$, similarly,

$$Z = \operatorname{tr}\left(e^{-\beta H}\right) = \lim_{M \to \infty} \operatorname{tr}\left[V^{M}(\phi)\right],\tag{6}$$

and

$$V(\phi) = 1 + \delta \sum_{\sigma} \left(\sum_{j=0}^{L-2} c_{j\sigma}^{\dagger} c_{j+1,\sigma} + e^{i\phi} c_{L-1,\sigma}^{\dagger} c_{0\sigma} + \text{h.c.} - \frac{U}{t} \sum_{j=0}^{L-1} n_{j\uparrow} n_{j\downarrow} \right). \quad (7)$$

We write $V^M(\phi) = \sum_{\alpha} X^{\alpha} = \sum_{\alpha} \prod_{\sigma} X^{\alpha}_{\sigma}$ as we rearrange the operator string by their spin indices. Then in Lieb's representation, we have $\operatorname{tr}(X) = \operatorname{tr}(\prod_{\sigma} X_{\sigma}) = \operatorname{tr}(X_{\uparrow}) \cdot \operatorname{tr}(X_{\downarrow})$. The lowest order nontrivial term with interactions $(-U/t)\delta \cdot \delta^L \cos \phi$ together with the purely kinetic contribution term $\delta^L \cos \phi$ gives $[1 + (-U/t)\delta]\delta^L \cos \phi$, which maximizes the same way as free fermions at any finite temperature. That is, at finite temperature, the optimal flux for the free energy of the 1D Hubbard model should not be affected by any finite Hubbard interaction. Numerical examples also confirm this as shown in figures 2(b), (d) and (f). However, the optimal flux for the zero-temperature ground state energy is altered by increasing the Hubbard interactions when it is not half-filled. Note that if $U \to \infty$, the above statement is not valid anymore since the sign of $[1 + (-U/t)\delta]$ is not well-defined any longer. One counter-example we already know is the Nagaoka state [60], which says that the Hubbard model with one fermion away from half-filling will fully polarize in the limit $U \to \infty$. Long-range hoppings or the 2D Hubbard model can induce the Nagaoka polarization with large but finite U/t [15].

- (b) Because of the GRP, the original system and the fictitious reflective system share the same flux to reach the maximum of the partition function at the same time. Thus the flux period reduces from 2π to π . Numerically we can also see this in figures 2(a), (c) and (e). $\phi = \pm \pi/2$ are both optimal fluxes but have opposite chiralities. The spin chiral order operator $\chi = \sigma_1 \cdot (\sigma_2 \times \sigma_3)$, which depends on the imaginary part of the gauge invariant Berry phases, will not only be nonzero but also maximized with respect to the optimal $\pm \pi/2$ fluxes. At the same time, nonvanishing charge currents $J_{ij} = i \sum_{\sigma} (c_{i\sigma}^{\dagger} c_{j\sigma} \text{h.c.})$ [16, 91] should be observed around the loop lattice. Both time-reversal symmetry \mathcal{T} and parity symmetry \mathcal{P} break spontaneously and chiral order emerges. However, the combined $\mathcal{P}\mathcal{T}$ -symmetry is not broken, which illustrates a kind of nonrelativistic PT theorem if U(1) symmetry is preserved [10].
- (c) This result reminds us of Haldane's honeycomb model [23] where there is a chiral $\pm \pi/2$ flux threaded through each second-neighboring triangle. It is energetically favored, and time-reversal symmetry \mathcal{T} and parity symmetry \mathcal{P} are spontaneously broken.

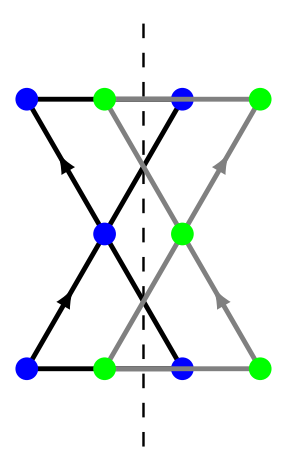


Figure 4. Carrying out the GRP along the dashed line on a bowtie lattice. Its fictitious reflection copy is illustrated by gray links.

2.3. Flux singularity as a Luttinger liquid signature

Another important issue to be addressed here is shown in figure 2, where the ground state energies always exhibit a nonanalytical singularity at $\phi = \pi$. This can be understood easily at least in a free particle picture. As shown in figure 1, in the momentum space since we have a discrete momentum step $\Delta k = 2\pi/L$, when the threaded flux ϕ is approaching π , the momentum shift behaves like $\delta k = \frac{\phi}{L} \to \frac{\pi}{L} = \frac{1}{2}\Delta k$. Therefore, there will be a sudden rearrangement of the particle fillings in terms of the two branches of fermions when ϕ steps across π . The finite-size energy gap closes at the same time. Note that this particular phenomenon stems from nothing but the very special dimensionality of 1D. In 1D, the Fermi surface shrinks to two disconnected Fermi points, which essentially make 1D fermions an NFL. As is well known, the low-energy physics of 1D fermions is described by the Luttinger liquid (LL) theory [22, 53, 82], which crucially differs from higher dimensions. There exist forbidden scattering regions and unrenormalizable gapless Fermi momenta [12, 22, 89]. In this sense, when we vary the threaded flux ϕ , these singularities can be regarded as a kind of Luttinger-like NFL smoking-gun evidence [42, 51]. As expected in LL, this flux singularity located at π is unchanged, even involving Hubbard interactions. When it is away from half-filling as shown in figures 2(b), (d) and (f), the flux singularity at $\phi = \pi$ is always located there, only its relative energy is changed by increasing Hubbard interactions. What we find more interesting is that—as shown in figure 2(f)—with very large U/t = 100.0, sufficiently strong Hubbard interactions can lead to some emergent flux singularities. We attribute these to the emergent Luttinger-like flux singularities driven by strong Hubbard interactions, which are absent in free or weakly interacting fermionic states. These states cannot also be adiabatically connected to the noninteracting fermions. As we can see, from the perspective of the flux issue, doping a half-filled Mott insulator with sufficiently large Hubbard interactions turns out to make the system dramatically different from the original parent [41]. These emergent flux singularities can only appear in doped cases away from half-filling.

3. Two-dimensional lattices

Most of our physical interest lies in 2D. High- $T_{\rm c}$ superconductivity is generally regarded as a 2D physical problem, where electrons are restricted within each single Cu–O plane [14, 41]. Free or weakly interacting fermions in 2D are described by Fermi-liquid theory, which is dramatically different from LL theory. There is a continuous Fermi surface and no singular scattering occurs. As a matter of fact, decades ago it had already been proposed by Anderson that strong interactions could lead to some Luttinger-like features in a 2D Hubbard model stemming from the unrenormalizable quantum phase shift and singular scatterings [4, 6]. When interactions are increased until they are sufficiently strong, Fermi-liquid theory will break down and singular scatterings within the Brillouin zone may occur.

3.1. A trial on a bowtie lattice

In 2D, let us begin with a kind of very simple lattice, namely a bowtie lattice consisting of five sites as illustrated in figure 4. As a generalization of the GRP on 1D rings, we have the following corollary:

Corollary 3.1. For a half-filled repulsive Hubbard model with a minimal $|S_{tot}^z|$ defined on a bowtie as in figure 4, at any finite temperature, the optimal fluxes for the free energy F are $\pm \pi/2$ in each triangle.

Proof. Carry on the GRP along the dashed line as illustrated in figure 4. The other procedures are the same with the 1D ring.

However, the GRP cannot tell us the sign of the fluxes in each triangle. Due to the fact that the GRP only requires a half-filled condition while it does not care about whether U=0.0 or not, we can thus deduce the flux pattern for interacting fermions from free fermions at half-filling. In other words, at half-filling, the (G)RP make a continuous connection between the Hubbard interacting fermions and free fermions. The optimal flux patterns are the same on both sides.

The optimal flux for free fermions on a bowtie at half-filling turns out to share the identical sign of $\pm \pi/2$. We verified this conclusion for interacting fermions by the numerical ED as shown in figure 5 and provide some more results deviating from half-filling as a comparison. We can see that on a 2D bowtie lattice, half-filling is still such a special filling that the free energy and ground state energy share the same optimal flux, which is immobile by changing the Hubbard interactions. Otherwise it is not when it is away from half-filling.

3.2. Triangular and Kagome lattices

Now we turn to the flux problem on more complicated 2D nonbipartite lattices, such as triangular and Kagome [20, 55, 74], in terms of free as well as Hubbard interacting fermions.

3.2.1. Half-filled free fermions coupled to a \mathbb{Z}_4 gauge field. We would like to consider the flux problem of half-filled free fermions both on the triangular and Kagome lattices

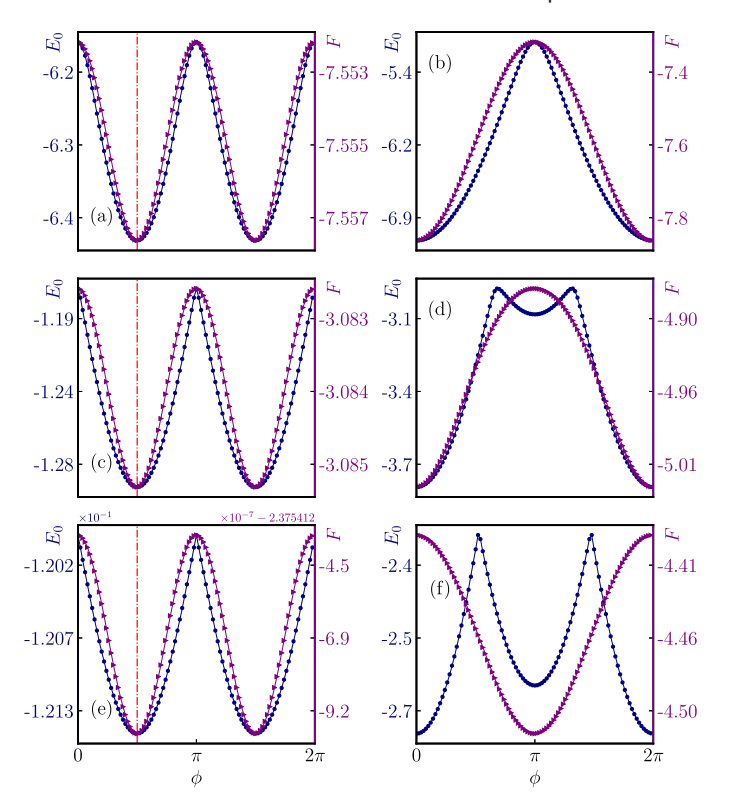


Figure 5. The ground state energy E_0 and the finite temperature free energy F of the Hubbard model on a bowtie lattice. Vertically, (a), (b), (c), (d) and (e), (f) denote U/t = 0.0, 10.0, 100.0, respectively. Horizontally, (a), (c), (e) denote half-filling $N_{\uparrow} = 3, N_{\downarrow} = 2$; (b), (d), (f) denote filling $N_{\uparrow} = N_{\downarrow} = 2$. Free energy is computed at $\beta = 1.0$. The red dashed line marks the optimal flux $\phi = \pi/2$ for the ground state at half-filling.

first. According to our previous discussions, here $\pm \pi/2$ fluxes are also strongly implied in the plaquettes encircled by odd-numbered links. Therefore, we would like to imagine that there is only a minimal $\mathbb{Z}_4 \subset \mathrm{U}(1)$ gauge field coupled to these lattice fermions. \mathbb{Z}_4 is the smallest gauge group that possibly supports $\pm \pi/2$ fluxes. A pure \mathbb{Z}_4 lattice gauge theory should take the form of

$$H_g = -\frac{J}{2} \sum_{p} \prod_{l \in p} \tau_l + \text{h.c.}, \tag{8}$$

where $\tau_l \in G = \{1, i, -1, -i\}$ is the gauge connection living on the link l of each plaquette p. G is our gauge group. J is the coupling constant. Generically, this \mathbb{Z}_4 gauge field can be coupled to lattice fermions through

$$H_f = -\sum_{\sigma} \sum_{\langle ij \rangle} (\tau_{ij} c_{i\sigma}^{\dagger} c_{j\sigma} + \text{h.c.}) + H_g + H_U.$$
(9)

Here for the free fermions with U = 0.0, we only consider the gauge field as a background, which means J = 0.0. The gauge field does not provide its own dynamics. Given

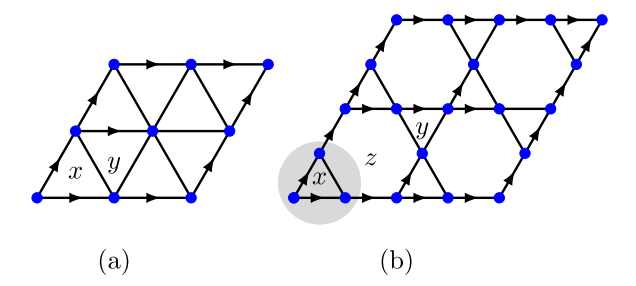


Figure 6. A 2×2 enlarged magnetic unit cell with respect to fixed gauge choices. An arrow denotes the gauge connection $\exp(+i\pi/2)$ fixed on this very link. (a) A triangular lattice with a flux state labelled by [x, y]. (b) A Kagome lattice with a flux state labelled by [x, y, z].

equation (9), exploring the whole phase diagram as well as the phase transitions would be quite an interesting task, which, however, deviates from the goal of this paper and will be left for the future.

Since the two branches $\sigma = \uparrow, \downarrow$ are decoupled and symmetric, if we are on a lattice with an even number of sites, we can only consider one of them and the Hamiltonian can be written as $H = \eta^{\dagger} \mathcal{H} \eta$ where $\eta = (c_0, c_1, \ldots, c_{N-1})^T$ assuming there are N sites consisting of the lattice. We should also assume that the magnetic unit cell can only be enlarged as much as 2×2 greater than the original lattice unit cell. The question remaining is to find out which flux pattern is optimal to make this fermion–gauge-field coupled system possess the lowest ground state energy.

For the triangular lattice as shown in figure 6(a), within the enlarged magnetic unit cell, we have a specific fixed gauge choice, as the arrows indicate, then leave the other seven links free. The undetermined gauge field connections without arrows can be chosen from the \mathbb{Z}_4 gauge group at liberty. In this sense, there are $\mathcal{N}=4^7=16\,384$ kinds of choice in total. We sought all these possibilities numerically on a 16×16 triangular lattice with periodic boundary conditions (PBC); $\pm [\pi/2, \pi/2]$ turn out to be the optimal flux patterns. For the Kagome lattice as shown in figure 6(b), within the enlarged magnetic unit cell, there are 11 free links determining various flux patterns. We sought all the $\mathcal{N}=4^{11}=4194\,304$ kinds of possibility numerically on a $4\times4\times3$ Kagome lattice with PBC; $\pm [\pi/2, \pi/2, 0]$ are the two optimal flux patterns for the Kagome lattice. Some representative flux states and their energy are enumerated in table 1. In figure 7 we also show the finite-size effect of the energy for these flux states. On both triangular and Kagome lattices, we can see that every rhomboid still prefers a π flux while a 0 flux gives much higher energy. Moreover, these optimal flux states converge more quickly. It seems that they are much less sensitive to the finite-size effect in comparison with other flux states.

3.2.2. Turn on Hubbard interactions. As a generalization of 1D rings and a 2D bowtie lattice, we can carry out the GRP along the dashed lines on these kinds of lattices, as shown in figure 8. Note that the direct application of our GRP is that every nonintersected link will acquire a pure imaginary gauge connection in order to maximize the partition function. In this sense, we can have the two following corollaries:

Table 1.	The per-site	energy of som	ne flux state	es for h	alf-filled	free	${\rm fermions}$	on	a
16×16 to	riangular latt	cice and a 8×8	8×3 Kagor	ne latti	ice with I	PBC.			

Tr	iangle	Kagome			
$\frac{1}{[+\pi/2, +\pi/2]}$	-1.20102	$[+\pi/2, +\pi/2, 0]$	-0.89912		
$[\pi,0]$	-1.18341	$[0,0,\pi]$	-0.88413		
$[+\pi/2, -\pi/2]$	-0.94263	$[+\pi/2, -\pi/2, 0]$	-0.85897		

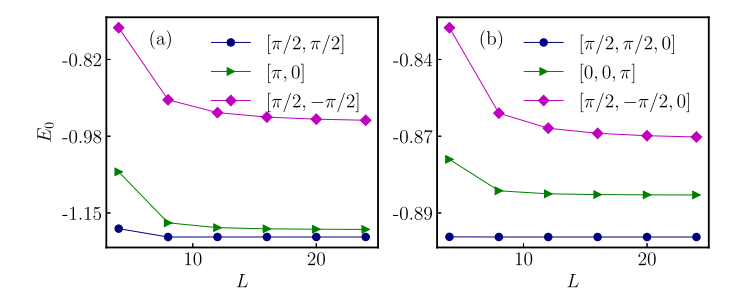


Figure 7. Finite-size scaling of the ground state energy for kinds of flux states on $L \times L$ lattices with PBC. (a) Triangular lattice. (b) Kagome lattice.

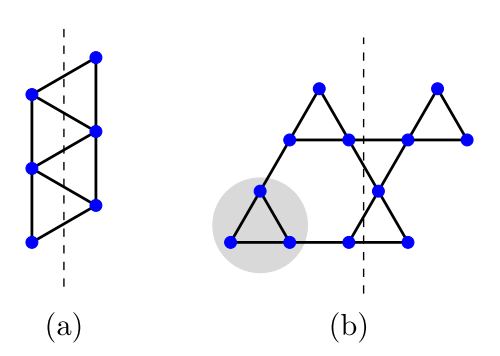


Figure 8. Carrying out the GRP on (a) a triangular lattice and (b) a Kagome lattice. Within a lattice unit cell (shadowed area) of the Kagome lattice there are three inequivalent sites.

Corollary 3.2. For a half-filled repulsive Hubbard model with a minimal $|S_{tot}^z|$ defined on a triangular lattice, the optimal fluxes for its free energy F at any finite temperature are $\pm \pi/2$ in each triangle.

Corollary 3.3. For a half-filled repulsive Hubbard model with a minimal $|S_{tot}^z|$ defined on the Kagome lattice, the optimal flux patterns for its free energy F at any finite temperature are $\pm \pi/2$ in each triangle and 0 or π in each hexagon.

On the one hand, if only based on the GRP, analytically we still cannot nail down the sign of the triangle flux $\pm \pi/2$ for the half-filled Hubbard interacting fermions on the triangular and Kagome lattices. Although Lieb's original result [47] implies that every

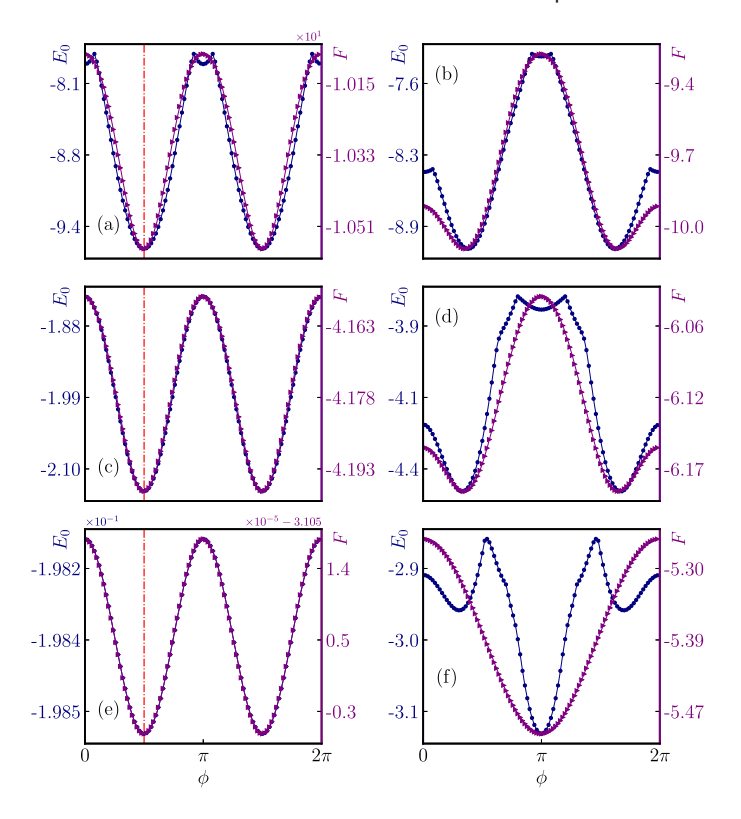


Figure 9. The ground state energy E_0 and finite temperature free energy F of the Hubbard model on a triangular lattice consisting of six sites. Vertically, (a), (b), (c), (d) and (e), (f) denote U/t = 0.0, 10.0, 100.0, respectively. Horizontally, (a), (c), (e) denote half-filling $N_{\uparrow} = N_{\downarrow} = 3$; (b), (d), (f) denote filling $N_{\uparrow} = 3, N_{\downarrow} = 2$. Free energy is computed at $\beta = 1.0$. The red dashed line marks the optimal flux $\phi = \pi/2$ for the ground state at half-filling.

rhomboid of a triangular lattice should prefer a π flux rather than 0, the RP cannot be directly applied here since we have an effective next-nearest neighbor hopping for each rhomboid. As we have mentioned, at the particular half-filling, the (G)RP can make a bridge between free and Hubbard interacting fermions. It does not matter whether Hubbard U is zero or not. On the other hand, our numerical study of free fermions coupled to a static \mathbb{Z}_4 gauge field on triangular and Kagome lattices has shown us the optimal flux patterns, but we still cannot state them as proof since we have imposed a magnetic unit cell assumption as well as a finite lattice size. Combining these two factors, we can at least strongly believe that the optimal flux patterns for the repulsive Hubbard model at half-filling are $\pm [\pi/2, \pi/2]$ and $\pm [\pi/2, \pi/2, 0]$ on the triangular and Kagome lattices, respectively.

For the triangular lattice, we have another argument: we can carry out the ordinary RP along the dashed line as illustrated in figure 8 with a *glide* geometric reflection $\widetilde{\mathcal{R}}$ instead of a direct geometric reflection \mathcal{R} , saying that every rhomboid of the triangular lattice prefers a π flux, which coincides with the optimal flux patterns $\pm [\pi/2, \pi/2]$.

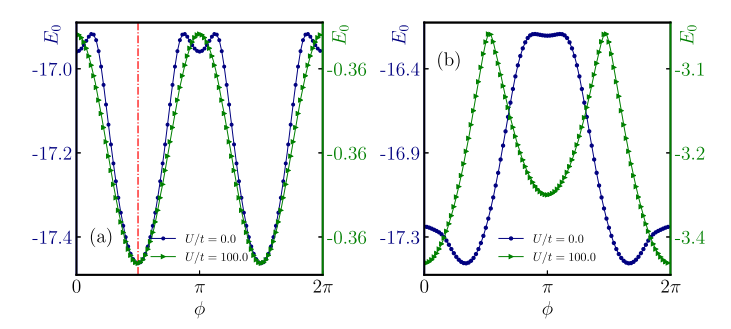


Figure 10. The ground state energy E_0 of the Hubbard model on a $2 \times 2 \times 3$ Kagome lattice with an open boundary condition. Flux ϕ is added through each triangle while there is no flux threading through the hexagon. (a) Refers to the half-filled $N_{\uparrow} = 6$, $N_{\downarrow} = 6$. The dashed line denotes $\pi/2$. (b) Refers to the Nagaoka filling $N_{\uparrow} = 6$, $N_{\downarrow} = 5$.

3.3. Numerical verification and flux singularities induced by strong Hubbard interactions

Meanwhile, we simulate the interacting fermions by the numerical ED on both triangular and Kagome lattices as shown in figures 9 and 10. Note that we cannot obtain the free energy for the Hubbard model up to N = 12 sites by ED but only the ground state energy because of the iterative algorithm [70].

On the Kagome lattice, the half-filled case shown in figure 10(a) is consistent with our previous discussion. The optimal flux pattern even up to U/t = 100.0 is still the same as the free fermions. For the Nagaoka filling, we can see that in figure 10(b) Hubbard interactions can dramatically change the optimal flux pattern. The optimal flux for free fermions is located at $\phi \simeq \pi/3$ there, while with U/t = 100.0, the ground state with minimal energy is located at $\phi = 0$.

For the triangular lattice, by ED we also numerically checked that the energy of flux state $[\pi/2, \pi/2]$ was lower than the state $[0, \pi]$ [68], which are both π -flux states in a rhomboid.

For the bowtie lattice, when it is away from half-filling as shown in figures 5(b), (d) and (f), there is no flux singularity for free fermions. But sufficiently strong Hubbard interactions can give birth to new emergent flux singularities as shown in figure 5(f). As discussed in 1D, we think that it is still quite reasonable to regard these very singularities as some emergent Luttinger-like NFL features driven by strong interactions in 2D [42, 76, 83]. On the Kagome lattice with a Nagaoka filling in figure 10(b), we have also numerically observed similar emergent flux singularities for U/t = 100.0. This is the Luttinger-like evidence in pure 2D, which contradicts Fermi-liquid theory.

4. Conclusion and discussion

4.1. Brief summary

In this paper, we did a systematic study on the flux problem of free as well as Hubbard interacting fermions on nonbipartite lattices. At half-filling, several rigorous results can

be proved by utilizing the GRP technique. Other fillings are studied numerically. On a 1D nonbipartite odd-numbered ring at half-filling, the optimal flux for the ground state is at an unrenormalized $\pm \pi/2$. While away from half-filling, the optimal flux can be altered by strong Hubbard interactions. In 2D at half-filling, the optimal flux of the Hubbard model on the triangular lattice, $\pm [\pi/2, \pi/2]$ states are ascertained as the lowest energy flux states. For the Kagome lattice, they are $\pm [\pi/2, \pi/2, 0]$. On both the triangular and Kagome lattice, the chiral order parameter for each triangle, namely $\sigma_1 \cdot (\sigma_2 \times \sigma_3)$, is not only nonvanishing but also maximized in the lowest energy optimal flux states. We also addressed and discussed the numerically observed emergent flux singularities driven by strong Hubbard interactions and attributed them to some Luttinger-like NFL features. It is easy and straightforward to generalize our results to the extended Hubbard model [46, 73] while we do not expatiate on it here. For other more complicated nonbipartite lattices, such as decorated honeycomb [50] and 3D lattices [11, 38], we still draw similar conclusions if we are in the same fermion—gauge-field scenario, meaning that $\pm \pi/2$ fluxes will possibly emerge from the plaquettes with odd-numbered sites.

So far, we can provide a basic answer to the question asked in the introduction section 1: if we lose bipartiteness, for the half-filled free as well as Hubbard interacting fermions coupled to appropriate gauge fields, time-reversal symmetry \mathcal{T} and parity symmetry \mathcal{P} break spontaneously. Chiral fermions will emerge. Ground states are not unique any longer. The sign problem cannot be avoided if simulated by quantum Monte Carlo.

4.2. Possible implication on quantum spin liquids

As we have mentioned, the fermion-gauge theory coupled scheme is not only a fantastic scenario but also quite realistic. A pure bosonic model can be written in terms of slave-fermions [2, 58]. Gauge fields can indeed emerge from these strongly correlated bosonic quantum systems.

In recent years, the Kagome lattice has attracted a great deal of attention with respect to the study of QSLs [9, 24, 25, 27, 29, 52, 69, 92]. On the projected mean-field level of slave-fermions, the Dirac state $[0,0,\pi]$ is always reported to serve as the parent state for various kinds of QSLs on the Kagome lattice [69]. However, in this paper we found that for not only free but also Hubbard interacting fermions at half-filling, the ground state energy of the flux states $\pm [\pi/2, \pi/2, 0]$ is lower than the Dirac state $[0,0,\pi]$. Although the ground state wavefunction of the Hubbard model is not equivalent to the Gutzwiller projected mean-field wavefunctions, we think it is still meaningful to study QSLs starting from the chiral $\pm [\pi/2, \pi/2, 0]$ states. As well as on the triangular lattice, these optimal flux states break time-reversal symmetry \mathcal{T} . Even up to very strong Hubbard interactions, we have demonstrated that the lowest energy ground state of these half-filled fermion—gauge-theory coupled systems always tends to select some $\pm \pi/2$ fluxes within the plaquettes enclosed by odd-numbered links.

In this sense, our results strongly imply that time-reversal symmetry breaking chiral fermions and chiral QSLs [10, 84] may be widely present as well as stabilized by emergent gauge fields in strongly correlated bosonic quantum systems on various kinds of frustrated nonbipartite lattices. Possible examples have been reported widely such as in

the references [13, 18, 19, 36, 62, 77, 78, 90]. Note, however, that an emergent \mathbb{Z}_2 gauge field can only allow a Dirac state which does not break time-reversal symmetry \mathcal{T} . If $\pm \pi/2$ fluxes are expected, the emergent gauge field must at least be a \mathbb{Z}_4 one. A U(1) gauge field is also possible but it is more subtle because of the possible confinement [43, 66, 88].

4.3. Outlook

So far we have studied lattice fermions on several kinds of nonbipartite lattices, especially at half-filling. We hope to continue to explore the fruitful features of strongly interacting fermions on nonbipartite lattices away from half-filling. For example, if one hole is doped, the Nagaoka state emerges on bipartite lattices if Hubbard interactions are sufficiently strong. However, as far as we know, we do not have much information for the Hubbard model with Nagaoka filling on nonbipartite lattices yet.

In the continuum limit, a field theoretical description is still needed. In 1D, the conventional bosonization technique can be applied to the system, which might lead to some new perspectives and physics. Furthermore, we also know that chiral spin states are deeply related to the topological Chern–Simons term in field theory, which breaks the parity symmetry \mathcal{P} and time-reversal symmetry \mathcal{T} simultaneously. Actually, fermion statistics can also be altered by the gauge fields [32, 59, 67], thus bosons and even anyons may emerge. Further discussion on the application of our current results towards quantum Hall effects [31, 37] and topological quantum field theories will hopefully be addressed in the future.

Acknowledgements

WZ would like to thank D N Sheng for her hospitality and helpful instructions at CSUN, California, where this work was inspired and initialized. WZ thanks Y M Lu, T L Ho, X Z Feng, Z Y Weng and A Rasmussen for many valuable discussions. WZ thanks the Referee for making several helpful suggestions to strengthen the revised manuscript. WZ also acknowledges Unity, a well-managed high-performance computing cluster in the College of Arts and Sciences of the Ohio State University. This work is supported by the National Science Foundation under award number DMR-1653769.

Appendix A. One-dimensional free spinless fermions and the Jordan-Wigner transformation

The Hamiltonian of spinless free fermions on such a lattice can be written as

$$H_0 = -\sum_{j=0}^{L-1} \left(t_{j,j+1} c_j^{\dagger} c_{j+1} + \text{h.c.} \right), \tag{10}$$

the Hamiltonian equation (10) becomes $H_0 = -\sum_k (2 \cos k) c_k^{\dagger} c_k$ if we set $t_{j,j+1} = 1.0$. Suppose there is a fixed number of $N(N \leq L)$ spinless fermions living on the ring and preserve the U(1) symmetry. Different boundary conditions will impose different

quantization conditions of k. For example, PBC gives $kL = 2l\pi$, $l \in \mathbb{Z}_+$. If N is even, there is a two-fold ground state degeneracy. The anti-periodic boundary condition gives $kL = (2l+1)\pi$, $l \in \mathbb{Z}_+$. If N is odd, there is a two-fold ground state degeneracy.

The ground state is simply the one in which the lowest N orbitals are occupied. More generally suppose there is a flux $\phi \in [0, 2\pi)$ threading the ring, we have the shifted $k = (2l\pi + \phi)/L$, $l \in \mathbb{Z}_+$. When it comes to the ground state(s), for N = 2n + 1, $n \in \mathbb{Z}_+$, the optimal flux is 0 since the lowest mode with k = 0 can be occupied by one fermion. For N = 2n, $n \in \mathbb{Z}_+$, the optimal flux is π for the sake of symmetric band filling.

On the other hand, we know that 1D spinless fermions can be exactly mapped to a spin model through the Jordan–Wigner transformation [34]. For j = 0, $c_0 = \sigma_0^-$, $c_0^{\dagger} = \sigma_0^+$; and for $j \ge 1$,

$$c_{j} = \left[\prod_{l=0}^{j-1} e^{i\pi\sigma_{l}^{+}\sigma_{l}^{-}}\right] \sigma_{j}^{-} = \left[\prod_{l=0}^{j-1} \left(-\sigma_{l}^{z}\right)\right] \sigma_{j}^{-}$$

$$c_{j}^{\dagger} = \sigma_{j}^{+} \left[\prod_{l=0}^{j-1} e^{-i\pi\sigma_{l}^{+}\sigma_{l}^{-}}\right] = \sigma_{j}^{+} \left[\prod_{l=0}^{j-1} \left(-\sigma_{l}^{z}\right)\right],$$

$$(11)$$

where $\sigma^{\pm} = (\sigma^x \pm i\sigma^y)/2$. $\sigma^{x,y,z}$ are the Pauli matrices. Specifically, a 1D spin-1/2 XY model reads

$$H_{XY} = -\sum_{j=0}^{L-1} \frac{1}{2} \left(t_{j,j+1} \sigma_j^x \sigma_{j+1}^x + \sigma_j^y \sigma_{j+1}^y \right)$$

$$= -\sum_{j=0}^{L-1} \left(t_{j,j+1} \sigma_j^+ \sigma_{j+1}^- + \text{h.c.} \right), \tag{12}$$

which is equivalent to a hard-core boson model

$$H_b = -\sum_{j}^{L-1} \left(t_{j,j+1} b_j^{\dagger} b_{j+1} + \text{h.c.} \right)$$
 (13)

if we identify $\sigma^+ \sim b^{\dagger}$, $\sigma^- \sim b$ as the creation and annihilation operators of the hard-core bosons. Assuming $t_{j,j+1}$ are real and $t_{j,j+1} > 0$, $\forall j$, these hard-core bosons are on a periodic ring without any flux inserted. Note that if we carry out the Jordan-Wigner transformation of these bosons, a boundary term will appear in the fermionic model like

$$H_{\text{JW}} = -\sum_{j=0}^{L-2} \left(t_{j,j+1} c_j^{\dagger} c_{j+1} + \text{h.c.} \right) + Q \left(t_{L-1,0} c_{L-1}^{\dagger} c_0 + \text{h.c.} \right), \tag{14}$$

where $Q = \prod_{j=0}^{L-1} \left(-\sigma_j^z\right) = (-)^{\sum_j c_j^{\dagger} c_j} = (-)^N$ is the parity operator. That is, if we require equations (14) and (13) to be exactly mapped to each other, the boundary condition for equation (14) must be compatible with the parity of fermions. If N is even, Q = +1 denoting that the Jordan–Wigner fermions have an anti-periodic boundary condition (APBC). In other words, a fictitious π -flux is effectively inserted through the ring. If

N is odd, Q = -1 denotes a PBC, which means a 0-flux is inserted through the ring. According to the natural inequality [63, 64] theorem, the ground state energy of these hard-core bosons will never be greater than spinless fermions if they share the same form of Hamiltonians like equations (13) and (10). If the parity is compatible with the boundary condition, meaning that the Jordan–Wigner transformation is exactly valid, equations (13) and (14) will have the same ground state energies, which means the lower bound of the natural inequality is touched. Thus we conclude that the optimal flux for spinless free fermions is π or 0 if the particle number is even or odd, respectively. In a word, the optimal flux states for spinless fermions should be nonchiral, which preserve the time reversal symmetry.

In the case of finite temperature and free energy $F = -1/\beta \ln Z$ with inversed temperature β , we have

Lemma 4. For free spinless fermions with the Hamiltonian defined by equation (10) on a ring lattice, at any finite temperature the optimal flux for free energy is identical to the optimal flux in its ground state, namely 0 or π depending on whether the parity of the particle number N is odd or even.

Proof. The canonical partition function reads

$$Z = \operatorname{tr}\left(e^{-\beta H_0}\right) = \lim_{M \to \infty} \operatorname{tr}\left[V^M(\phi)\right],\tag{15}$$

and

$$V(\phi) = 1 + \delta \left(\sum_{j=0}^{L-2} c_j^{\dagger} c_{j+1} + e^{i\phi} c_{L-1}^{\dagger} c_0 + \text{h.c.} \right), \tag{16}$$

where we have chosen a specific gauge and defined $\delta \equiv t\beta/M$. For a fixed M, $V^{M}(\phi)$ can be expanded to a polynomial as $V^{M}(\phi) = \sum_{\alpha} X_{\alpha}$, where X_{α} is a string of fermionic operators. First of all, we make it a convention to label all the lattice sites in a 1D array and then write the basis of the Hilbert space as $|\alpha\rangle \equiv \{c^{\dagger}c^{\dagger}\cdots|0\rangle\}$ with a fixed order of lattice fermions. The nonvanishing tr(X) requires that X must recover a basis configuration to itself. In this sense, there are two kinds of operator strings: trivial ones such as 1 and $c_0^{\dagger}c_{L-1}c_{L-1}^{\dagger}c_0$ whose contributions are identical to the zero-flux partition function's, and nontrivial ones so long as X translates at least one fermion winding along the ring to acquire a phase $e^{\pm i\phi}$. Note that the most significant nontrivial operator string is to translate one fermion once around the ring as taking the order of δ^L . If $N=2n+1, n\in\mathbb{Z}_+$, the number of fermions being crossed is even, and the fermion sign does not arise there. Therefore, this kind of term takes the form $(+e^{i\phi} + e^{-i\phi})\delta^L =$ $+2\delta^L\cos\phi$, which maximizes at $\phi=0$. The higher order nontrivial terms looking like $+2\delta^{2L}\cos(2\phi), +2\delta^{3L}\cos(3\phi), \cdots$ maximize with the same ϕ . If $N=2n, n\in\mathbb{Z}_+$, thus the number of fermions being crossed is odd. Therefore, an extra fermion sign will arise and this kind of term takes the form $(-e^{i\phi} - e^{-i\phi})\delta^L = -2\delta^L \cos \phi$, which maximizes at $\phi = \pi$. The higher order nontrivial contributing terms like $+2\delta^{2L}\cos(2\phi), -2\delta^{3L}\cos(3\phi), \cdots$ which maximize with the same ϕ . Once the partition function is maximized, the corresponding free energy is minimized.

Appendix B. Half-filled spin-1/2 free fermions on a nonbipartite odd-numbered ring

Firstly, let us suppose L = 4n + 1, $n \in \mathbb{Z}_+$. $N_{\uparrow} = 2n + 1$, $N_{\downarrow} = 2n$. There is $\phi > 0$ threaded through the ring and the corresponding momentum shift is ϕ/L . The ground state energy of the fermions around this local minimum can be expressed as

$$E_{0\uparrow} = -2t \cos\left(\frac{\phi}{L}\right) - 2t \sum_{l=1}^{n} \cos\left(\frac{2l\pi - \phi}{L}\right) - 2t \sum_{l=1}^{n} \cos\left(\frac{2l\pi + \phi}{L}\right),$$

$$E_{0\downarrow} = -2t \cos\left(\frac{\phi}{L}\right) - 2t \sum_{l=1}^{n} \cos\left(\frac{2l\pi - \phi}{L}\right) - 2t \sum_{l=1}^{n-1} \cos\left(\frac{2l\pi + \phi}{L}\right).$$
(17)

 $E_0 = E_{0\uparrow} + E_{0\downarrow}$. $\partial E_0/\partial \phi = 0$ gives

$$2 \sin\left(\frac{\phi}{L}\right) - 2\sum_{l=1}^{n} \sin\left(\frac{2l\pi - \phi}{L}\right) + 2\sum_{l=1}^{n} \sin\left(\frac{2l\pi + \phi}{L}\right) - \sin\left(\frac{2n\pi + \phi}{L}\right) = 0, \quad (18)$$

which is accidentally filled with $\phi = \pi/2$ no matter what L is. Note that we have the equation

$$2 \sin\left(\frac{\pi}{8n+2}\right) + 4 \sin\left(\frac{\pi}{8n+2}\right) \sum_{l=1}^{n} \cos\left(\frac{2l\pi}{4n+1}\right) = 1,$$
 (19)

which always holds. Secondly, let us suppose $L=4n+3, n \in \mathbb{Z}_+$. $N_{\uparrow}=2n+2, N_{\downarrow}=2n+1$. Their ground state energies are given by

$$E_{0\uparrow} = -2t \cos\left(\frac{\phi}{L}\right) - 2t \sum_{l=1}^{n+1} \cos\left(\frac{2l\pi - \phi}{L}\right) - 2t \sum_{l=1}^{n} \cos\left(\frac{2l\pi + \phi}{L}\right),$$

$$E_{0\downarrow} = -2t \cos\left(\frac{\phi}{L}\right) - 2t \sum_{l=1}^{n} \cos\left(\frac{2l\pi - \phi}{L}\right) - 2t \sum_{l=1}^{n} \cos\left(\frac{2l\pi + \phi}{L}\right).$$
(20)

 $E_0 = E_{0\uparrow} + E_{0\downarrow}$. $\partial E_0/\partial \phi = 0$ gives

$$2 \sin\left(\frac{\phi}{L}\right) - 2\sum_{l=1}^{n} \sin\left(\frac{2l\pi - \phi}{L}\right) + 2\sum_{l=1}^{n} \sin\left(\frac{2l\pi + \phi}{L}\right) - \sin\left[\frac{2(n+1)\pi - \phi}{L}\right] = 0,$$
(21)

which is still filled with $\phi = \pi/2$ no matter what L is. Note that the equation

$$2 \sin\left(\frac{\pi}{8n+6}\right) + 4 \sin\left(\frac{\pi}{8n+6}\right) \sum_{l=1}^{n} \cos\left(\frac{2l\pi}{4n+3}\right) = 1$$
 (22)

always holds. $\phi = -\pi/2$ follows a similar procedure. Thus in a word, as long as L > 1 and L is odd, the optimal fluxes for the ground state of half-filled free spin-1/2 fermions

are $\pm \pi/2$, which are independent of L finite or not. In reference [47] we find a similar result while we use different methods.

We can also compute the partition function in the momentum space,

$$Z = \operatorname{tr}\left(e^{-\beta H}\right) = \sum_{\alpha} \langle \alpha | e^{\frac{2\beta t \sum_{\sigma} \sum_{k} \cos k c_{k\sigma}^{\dagger} c_{k\sigma}}{k}} | \alpha \rangle$$

$$= \sum_{\gamma,\eta} \langle \gamma |_{\uparrow} e^{\frac{2\beta t \sum_{k} \cos k c_{k\uparrow}^{\dagger} c_{k\uparrow}}{k}} | \gamma \rangle_{\uparrow} \cdot \langle \eta |_{\downarrow} e^{\frac{2\beta t \sum_{k} \cos k c_{k\downarrow}^{\dagger} c_{k\downarrow}}{k}} | \eta \rangle_{\downarrow}$$

$$= \left(\sum_{\gamma} \langle \gamma | e^{\frac{2\beta t \sum_{k} \cos k c_{k}^{\dagger} c_{k}}{k}} | \gamma \rangle\right) \cdot \left(\sum_{\eta} \langle \eta | e^{\frac{2\beta t \sum_{k} \cos k' c_{k\downarrow}^{\dagger} c_{k'}}{k'}} | \eta \rangle\right), \tag{23}$$

where we have written a basis as $|\alpha\rangle=|\gamma\rangle_{\uparrow}\otimes|\eta\rangle_{\downarrow}$, of which the Hilbert space dimension is $D=C_L^{N_{\uparrow}}\cdot C_L^{N_{\downarrow}}$.

Appendix C. Other fillings on the triangular lattice

Here we compute more cases with different fillings of the Hubbard model on the triangular lattice as shown in figure C1.

Appendix D. Review of the reflection positivity on a bipartite lattice

Following the reference [46], on a bipartite graph Λ , the kinetic energy can be defined as

$$K = -\sum_{ij,\sigma} t_{ij} c_{i\sigma}^{\dagger} c_{j\sigma}. \tag{24}$$

The hopping amplitude satisfies $t_{ij} = t_{ji}^*$, thus the hopping matrix is Hermitian $T = T^{\dagger}$, and the Hubbard term

$$W = \sum_{j} U_{j} \left(n_{j\uparrow} - \frac{1}{2} \right) \left(n_{j\downarrow} - \frac{1}{2} \right). \tag{25}$$

The Hamiltonian is H=K+W. The Hamiltonian can be written as $H=H_L+H_R+H_I$. $H_I=t_{lr}c_l^{\dagger}c_r+t_{rl}c_r^{\dagger}c_l$. We are at liberty to choose $t_{lr}=t_{rl}$. Particle-hole transformation is defined as $\tau c_{i\sigma}\tau^{-1}=c_{i\sigma}^{\dagger}$ and we can find that $\tau(t_{ij}c_i^{\dagger}c_j)\tau^{-1}=t_{ij}c_ic_j^{\dagger}=-t_{ji}^*c_j^{\dagger}c_i$, which implies

$$\tau K(T)\tau^{-1} = K(-T^*). \tag{26}$$

Consider the so-called operator reflection Θ combined by three transformations:

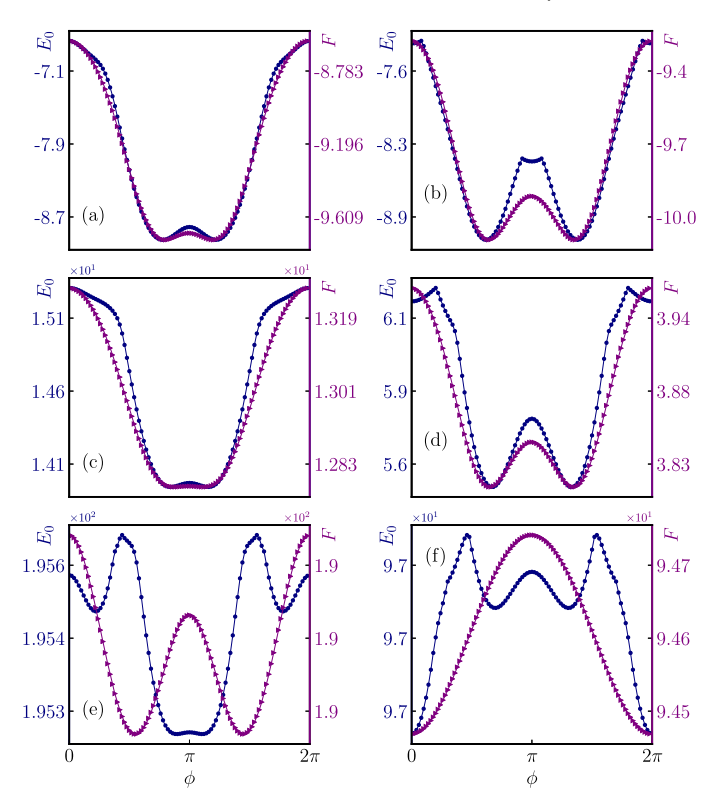


Figure C1. The ground state energy E_0 and the finite temperature free energy F of the Hubbard model on a triangular lattice consisting of six sites. Vertically, (a), (b), (c), (d) and (e), (f) denote U/t = 0.0, 10.0, 100.0, respectively. Horizontally, (a), (c), (e) denote half-filling $N_{\uparrow} = N_{\downarrow} = 4$; (b), (d), (f) denote filling $N_{\uparrow} = 4, N_{\downarrow} = 3$. Free energy is computed at $\beta = 1.0$.

- (a) Geometric reflection \mathcal{R} .
- (b) Particle-hole transformation τ .
- (c) Complex conjugation C, which only operates on the complex amplitude. For instance,

$$\Theta(t_{ij}c_i^{\dagger}c_j) = \mathcal{C}\left[\tau(t_{i'j'}c_{i'}^{\dagger}c_{j'})\tau^{-1}\right] = \mathcal{C}\left(-t_{j'i'}^*c_{j'}^{\dagger}c_{i'}\right) = -t_{j'i'}c_{j'}^{\dagger}c_{i'}.$$
(27)

Reflection positivity. Using the Trotter expansion we have

$$Z = \operatorname{tr}\left(e^{-\beta H}\right) = \lim_{M \to \infty} \operatorname{tr}\left(V^{M}\right) = \lim_{M \to \infty} \operatorname{tr}\left[\left(V_{I} V_{L} V_{R}\right)^{M}\right],\tag{28}$$

where $V_I=1-\beta H_I/M$, $V_L=\exp\left(-\beta H_L/M\right)$, $V_R=\exp\left(-\beta H_R/L\right)$. Note that $[V_L,V_R]=0$. Expanding $V^M=\sum_{\alpha}X^{\alpha}$, each term has the form $X=a_0\,V_L\,V_R\,a_1\,V_L\,V_R\ldots\,a_{M-1}\,V_L\,V_R$. a_i can be one of the three items $\mathbbm{1},\,c_l^{\dagger}c_r,\,-c_lc_r^{\dagger}$. Our strategy is to move all the left operators to the left without changing the order of the left operators themselves. One of the major difficulties here is that $c_l^\#$ operators have to move through $c_r^\#$.

Because of particle number conservation (V_L , V_R already conserve the particle on each side), the number of factor $c_l^{\dagger}c_r$ must be equal to the number $c_lc_r^{\dagger}$, otherwise $\operatorname{tr}(X) = 0$. In other words, the density matrix can be represented in the particle-hole symmetric reduced sub-Hilbert space. Denote the number of pairs $c_l^{\dagger}c_r$, $c_lc_r^{\dagger}$ in the sequence X as N. The first $c_l^{\#}$ moves through zero $c_r^{\#}$. The second moves through one. Thus the total number of induced fermion signs is $0 + 1 + 2 \cdots + (2N) = 2N^2$, which cancels the fermion sign.

X can be rewritten as $X = X_L \otimes X_R$. Then $\operatorname{tr}(X) = \operatorname{tr}(X_L) \cdot \operatorname{tr}(X_R)$, and $\operatorname{tr}(X_L)^* = \operatorname{tr}[\Theta(X_L)]$ since particle-hole transformation will not change the Hamiltonian. Thus we have $|\operatorname{tr}(X_L)|^2 = \operatorname{tr}(X_L) \cdot \operatorname{tr}(X_L)^* = \operatorname{tr}(X_L) \cdot \operatorname{tr}[\Theta(X_L)] = \operatorname{tr}[X_L \otimes \Theta(X_L)]$. Finally,

$$|\operatorname{tr}(V^{M})|^{2} = \left| \sum_{\alpha} \operatorname{tr}(X^{\alpha}) \right|^{2} = \left| \sum_{\alpha} \operatorname{tr}(X_{L}^{\alpha}) \cdot \operatorname{tr}(X_{R}^{\alpha}) \right|^{2}$$

$$\leq \sum_{\alpha} \left| \operatorname{tr}(X_{L}^{\alpha}) \right|^{2} \sum_{\beta} \left| \operatorname{tr}(X_{R}^{\beta}) \right|^{2}$$

$$= \sum_{\alpha} \operatorname{tr}\left[X_{L}^{\alpha} \otimes \Theta(X_{L}^{\alpha}) \right] \sum_{\beta} \operatorname{tr}\left[X_{R}^{\beta} \otimes \Theta(X_{R}^{\beta}) \right]. \tag{29}$$

Then we have

Lemma 5. For each $\beta \geqslant 0$ with fixed K_I ,

$$Z(H_L, H_R)^2 \leqslant Z[H_L, \Theta(H_L)] \cdot Z[H_R, \Theta(H_R)]. \tag{30}$$

Theorem 6. Assume $|t_{ij}|$ are Θ reflection invariant. Z is maximized by putting flux π in each square face of Λ .

References

- [1] 2013 The Hubbard model at half a century Nat. Phys. 9 523
- [2] Affleck I and Brad Marston J 1988 Large-n limit of the Heisenberg-Hubbard model: Implications for high- T_c superconductors $Phys.\ Rev.\ B$ 37 3774–7
- [3] Anderson P W 1972 More is different Science 177 393-6
- [4] Anderson P W 1990 "Luttinger-liquid" behavior of the normal metallic state of the 2d Hubbard model Phys. Rev. Lett. 64 1839-41
- [5] Anderson P W 1997 The Theory of Superconductivity in the High-T_c Cuprate Superconductors 1st edn (Princeton, NJ: Princeton University Press)
- [6] Anderson P W 1990 Singular forward scattering in the 2d Hubbard model and a renormalized Bethe ansatz ground state *Phys. Rev. Lett.* **65** 2306–8
- [7] Baskaran G and Anderson P W 1988 Gauge theory of high-temperature superconductors and strongly correlated Fermi systems Phys. Rev. B 37 580-3
- [8] Baskaran G, Zou Z and Anderson P W 1987 The resonating valence bond state and high- t_c superconductivity—a mean field theory *Solid State Commun.* **63** 973–6
- [9] Bauer B, Cincio L, Keller B P, Dolfi M, Vidal G, Trebst S and Ludwig A W W 2014 Chiral spin liquid and emergent anyons in a Kagome lattice Mott insulator Article Nat. Commun. 5 5137
- [10] Bieri S, Lhuillier C and Messio L 2016 Projective symmetry group classification of chiral spin liquids Phys. Rev. B 93 094437
- [11] Canals B and Lacroix C 1998 Pyrochlore antiferromagnet: A three-dimensional quantum spin liquid *Phys. Rev. Lett.* **80** 2933–6

- [12] Caux J-S and Smith C M 2017 Celebrating Haldane's 'Luttinger liquid theory' J. Phys.: Condens. Matter. 29 151001
- [13] Chen G, Kaden R, Hazzard A, Rey A M and Hermele M 2016 Synthetic-gauge-field stabilization of the chiralspin-liquid phase Phys. Rev. A 93 061601
- [14] Dagotto E 1994 Correlated electrons in high-temperature superconductors Rev. Mod. Phys. 66 763-840
- [15] Farkašovský P 2014 Ferromagnetism in the one-dimensional Hubbard model with long-range electron hopping and long-range Coulomb interaction Europhys. Lett. 107 57010
- [16] Fye R M, Martins M J, Scalapino D J, Wagner J and Hanke W 1991 Drude weight, optical conductivity, and flux properties of one-dimensional Hubbard rings Phys. Rev. B 44 6909–15
- [17] Gazit S, Randeria M and Vishwanath A 2017 Emergent Dirac fermions and broken symmetries in confined and deconfined phases of z₂ gauge theories Nat. Phys. 13 484
- [18] Gong S-S, Zheng W, Lee M, Lu Y-M and Sheng D N 2019 Chiral spin liquid with spinon Fermi surfaces in the spin- $\frac{1}{2}$ triangular Heisenberg model *Phys. Rev.* B **100** 241111
- [19] Gong S-S, Zhu W and Sheng D N 2014 Emergent chiral spin liquid: Fractional quantum Hall effect in a Kagome Heisenberg model Sci. Rep. 4 6317
- [20] Guertler S 2014 Kagome lattice Hubbard model at half filling Phys. Rev. B 90 081105
- [21] Gutzwiller M C 1963 Effect of correlation on the ferromagnetism of transition metals Phys. Rev. Lett. 10 159-62
- [22] Haldane F D M 1981 'Luttinger liquid theory' of one-dimensional quantum fluids. i. Properties of the Luttinger model and their extension to the general 1d interacting spinless Fermi gas J. Phys. C: Solid State Phys. 14 2585
- [23] Haldane F D M 1988 Model for a quantum Hall effect without Landau levels: Condensed-matter realization of the 'parity anomaly' Phys. Rev. Lett. 61 2015-8
- [24] Yin-Chen He D N S and Chen Y 2014 Chiral spin liquid in a frustrated anisotropic Kagome Heisenberg model Phys. Rev. Lett. 112 137202
- [25] Yin-Chen H, Zaletel M P, Oshikawa M and Frank P 2017 Signatures of Dirac cones in a DMRG study of the Kagome Heisenberg model *Phys. Rev.* X **7** 031020
- [26] Hirsch J E 1985 Two-dimensional Hubbard model: Numerical simulation study Phys. Rev. B 31 4403-19
- [27] Hu W-J, Zhu W, Zhang Y, Gong S, Becca F and Sheng D N 2015 Variational Monte Carlo study of a chiral spin liquid in the extended Heisenberg model on the Kagome lattice Phys. Rev. B 91 041124
- [28] Hubbard J and Flowers B H 1963 Electron correlations in narrow energy bands Proc. R. Soc. A 276 238-57
- [29] Iqbal Y, Becca F and Poilblanc D 2011 Projected wave function study of \mathbb{Z}_2 spin liquids on the Kagome lattice for the spin- $\frac{1}{2}$ quantum Heisenberg antiferromagnet *Phys. Rev.* B **84** 020407
- [30] Jaksch D and Zoller P 2005 The cold atom Hubbard toolbox Ann. Phys., NY 315 52-79
- [31] Kalmeyer V and Laughlin R B 1987 Equivalence of the resonating-valence-bond and fractional quantum Hall states *Phys. Rev. Lett.* **59** 2095–8
- [32] Karch A and Tong D 2016 Particle-vortex duality from 3d bosonization Phys. Rev. X 6 031043
- [33] Kitaev A 2006 Anyons in an exactly solved model and beyond Ann. Phys., NY 321 2-111
- [34] Kogut J B 1979 An introduction to lattice gauge theory and spin systems Rev. Mod. Phys. 51 659-713
- [35] Kotliar G 1988 Resonating valence bonds and d-wave superconductivity Phys. Rev. B 37 3664-66
- [36] Lai H-H 2013 Possible uniform-flux chiral spin liquid states in the SU(3) ring-exchange model on the triangular lattice *Phys. Rev.* B **87** 205111
- [37] Laughlin R B 1983 Anomalous quantum Hall effect: An incompressible quantum fluid with fractionally charged excitations *Phys. Rev. Lett.* **50** 1395–8
- [38] Lawler M J, Paramekanti A, Kim Y B and Leon B 2008 Gapless spin liquids on the three-dimensional hyperkagome lattice of na₄ir₃o₈ Phys. Rev. Lett. **101** 197202
- [39] LeBlanc J P F et al 2015 Solutions of the two-dimensional Hubbard model: Benchmarks and results from a wide range of numerical algorithms Phys. Rev. X 5 041041
- [40] Lee P A and Nagaosa N 1992 Gauge theory of the normal state of high- t_c superconductors *Phys. Rev.* B **46** 5621-39
- [41] Lee P A, Nagaosa N and Wen X-G 2006 Doping a Mott insulator: Physics of high-temperature superconductivity Rev. Mod. Phys. 78 17–85
- [42] Lee S-S 2018 Recent developments in non-Fermi liquid theory Annu. Rev. Condens. Matter Phys. 9 227-44
- [43] Lee S-S and Lee P A 2005 Emergent U(1) gauge theory with fractionalized boson/fermion from the Bose condensation of excitons in a multiband insulator *Phys. Rev.* B **72** 235104
- [44] Levin M and Wen X-G 2003 Fermions, strings, and gauge fields in lattice spin models Phys. Rev. B 67 245316
- [45] Lieb E H 1989 Two theorems on the Hubbard model Phys. Rev. Lett. 62 1201-4
- [46] Lieb E H 1994 Flux phase of the half-filled band Phys. Rev. Lett. 73 2158-61

- [47] Lieb E H and Loss M 1993 Fluxes, Laplacians, and Kasteleyn's theorem Duke Math. J. 71 337-63
- [48] Lieb E H and Wu F Y 1968 Absence of Mott transition in an exact solution of the short-range, one-band model in one dimension Phys. Rev. Lett. 20 1445–8
- [49] Lieb E H and Wu F Y 2003 The one-dimensional Hubbard model: a reminiscence Physica A 321 1-27
- [50] Lin H-F, Chen Y-H, Liu H-D, Tao H-S and Liu W-M 2014 Mott transition and antiferromagnetism of cold fermions in the decorated honeycomb lattice Phys. Rev. A 90 053627
- [51] Löhneysen H v., Rosch A, Vojta M and Peter W 2007 Fermi-liquid instabilities at magnetic quantum phase transitions Rev. Mod. Phys. **79** 1015–75
- [52] Lu Y-M, Ran Y and Lee P A 2011 \mathbb{Z}_2 spin liquids in the $s = \frac{1}{2}$ Heisenberg model on the Kagome lattice: a projective symmetry-group study of Schwinger fermion mean-field states *Phys. Rev.* B **83** 224413
- [53] Luttinger J M 1963 An exactly soluble model of a many-fermion system J. Math. Phys. 4 1154
- [54] Macris N and Bruno N 1996 On the flux phase conjecture at half-filling: An improved proof J. Stat. Phys. 85 745-61
- [55] Marston J B and Zeng C 1991 Spin-Peierls and spin-liquid phases of Kagomé quantum antiferromagnets J. Appl. Phys. 69 5962-4
- [56] Mazurenko A et al 2017 A cold-atom Fermi-Hubbard antiferromagnet Nature 545 462
- [57] Meng Z Y, Lang T C, Wessel S, Assaad F F and Muramatsu A 2010 Quantum spin liquid emerging in two-dimensional correlated Dirac fermions *Nature* **464** 847
- [58] Mudry C and Fradkin E 1994 Separation of spin and charge quantum numbers in strongly correlated systems $Phys.\ Rev.\ B\ 49\ 5200-19$
- [59] Murugan J and Nastase H 2017 Particle-vortex duality in topological insulators and superconductors J. High Energy Phys. JHEP05(2017)159
- [60] Nagaoka Y 1966 Ferromagnetism in a narrow, almost half-filled s band Phys. Rev. 147 392-405
- [61] Nakano F 2000 The flux phase problem on the ring J. Phys. A: Math. Gen. 33 5429-33
- [62] Nataf P, Lajkó M, Alexander W, Penc K, Mila F and Läuchli A M 2016 Chiral spin liquids in triangular-lattice SU(n) fermionic Mott insulators with artificial gauge fields Phys. Rev. Lett. 117 167202
- [63] Nie W, Katsura H and Oshikawa M 2013 Ground-state energies of spinless free fermions and hard-core bosons Phys. Rev. Lett. 111 100402
- [64] Nie W, Katsura H and Oshikawa M 2018 Particle statistics, frustration, and ground-state energy Phys. Rev. B 97 125153
- [65] Osterwalder K and Seiler E 1978 Gauge field theories on a lattice Ann. Phys., NY 110 440-71
- [66] Polyakov A M 1977 Quark confinement and topology of gauge theories Nucl. Phys. B 120 429-58
- [67] Polyakov A M 1988 Fermi-Bose transmutations induced by gauge fields Mod. Phys. Lett. A 03 325-8
- [68] Rachel S, Laubach M, Reuther J and Thomale R 2015 Quantum paramagnet in a π flux triangular lattice Hubbard model *Phys. Rev. Lett.* **114** 167201
- [69] Ran Y, Hermele M, Lee P A and Wen X-G 2007 Projected-wave-function study of the spin-1/2 Heisenberg model on the Kagomé lattice *Phys. Rev. Lett.* **98** 117205
- [70] Reuter M, Gomes F M and Sorensen D BSD Arpackpp Package (https://github.com/m-reuter/arpackpp)
- [71] Sachdev S 2016 Emergent gauge fields and the high-temperature superconductors *Phil. Trans. R. Soc.* A **374** 20150248
- [72] Sachdev S 2018 Topological order, emergent gauge fields, and Fermi surface reconstruction Rep. Prog. Phys. 82 014001
- [73] Sandvik A W, Leon B and Campbell D K 2004 Ground state phases of the half-filled one-dimensional extended Hubbard model Phys. Rev. Lett. 92 236401
- [74] Sasaki K and Takao M 2014 Dirac fermion state with real space π -flux on anisotropic square lattice and triangular lattice J. Phys. Soc. Japan 83 034712
- [75] Sorella S, Otsuka Y and Yunoki S 2012 Absence of a spin liquid phase in the Hubbard model on the honeycomb lattice Sci. Rep. 2 992
- [76] Stewart G R 2001 Non-Fermi-liquid behavior in d- and f-electron metals Rev. Mod. Phys. 73 797-855
- [77] Szasz A, Motruk J, Zaletel M P and Moore J E 2020 Chiral spin liquid phase of the triangular lattice Hubbard model: a density matrix renormalization group study Phys. Rev. X 10 021042
- [78] Taguchi Y, Oohara Y, Yoshizawa H, Nagaosa N and Tokura Y 2001 Spin chirality, Berry phase, and anomalous Hall effect in a frustrated ferromagnet Science 291 2573-6
- [79] Tarruell L and Sanchez-Palencia L 2018 Quantum simulation of the Hubbard model with ultracold fermions in optical lattices C. R. Phys. 19 365–93
- [80] Tasaki H 1995 The Hubbard Model: Introduction and Selected Rigorous Results (arXiv:cond-mat/9512169)

Fermi-Hubbard model on nonbipartite lattices: flux problem and emergent chirality

- [81] Thomson A and Sachdev S 2018 Fermionic spinon theory of square lattice spin liquids near the Néel state Phys. Rev. X 8 011012
- [82] Tomonaga S-I 1950 Remarks on Bloch's method of sound waves applied to many-fermion problems Prog. Theor. Phys. 5 544-69
- [83] Varma C M, Nussinov Z and van Saarloos W 2002 Singular or non-Fermi liquids Phys. Rep. 361 267-417
- [84] Wen X G, Frank W and Zee A 1989 Chiral spin states and superconductivity Phys. Rev. B 39 11413-23
- [85] Wen X G 2004 Oxford graduate texts Quantum Field Theory of Many-Body Systems: From the Origin of Sound to an Origin of Light and Electrons: From the Origin of Sound to an Origin of Light and Electrons (Oxford: Oxford University Press)
- [86] Wen X-G 2002 Quantum orders and symmetric spin liquids *Phys. Rev.* B **65** 165113
- [87] White S R, Scalapino D J, Sugar R L, Loh E Y, Gubernatis J E and Scalettar R T 1989 Numerical study of the two-dimensional Hubbard model *Phys. Rev.* B **40** 506–16
- [88] Xu X Y, Qi Y, Zhang L, Assaad F F, Xu C and Meng Z Y 2019 Monte Carlo study of lattice compact quantum electrodynamics with fermionic matter: The parent state of quantum phases *Phys. Rev.* X 9 021022
- [89] Yamanaka M, Oshikawa M and Affleck I 1997 Nonperturbative approach to Luttinger's theorem in one dimension Phys. Rev. Lett. 79 1110-3
- [90] Yao H and Kivelson S A 2007 Exact chiral spin liquid with non-abelian anyons Phys. Rev. Lett. 99 247203
- [91] Zheng W, Zheng Z, Sheng D N and Weng Z-Y 2018 Hidden spin current in doped Mott antiferromagnets Phys. Rev. B 98 165102
- [92] Zhu W, Chen X, Yin-Chen H and Witczak-Krempa W 2018 Entanglement signatures of emergent Dirac fermions: Kagome spin liquid and quantum criticality Sci. Adv. 4 eaat5535